Rotation curves of spiral galaxies as a consequence of a natural physical mechanism?

M. Kurpiewski
Szczecin, Poland
marek.qrp@gmail.com

ABSTRACT

Rotation curves of spiral galaxies for baryonic masses, which are inconsistent with the law of gravity, constitute one of the pillars of the dark matter concept. This publication shows that the effects attributed to the influence of dark matter in spiral galaxies, are extremely similar to effects of a certain physical mechanism, which has been noticed during the analysis of this problem.

Subject headings: galaxies: kinematics and dynamics – cosmology: dark matter

1. Introduction

Analysis of the inconsistency between rotation curves of spiral galaxies and the law of gravity (e.g. Rubin et al. 1978) revealed, that it is possible for a physical effect to occur, a natural consequence of which is the observed increase in velocity of a particle located in the gravitational field. The concept that uses it to explain the non-compliance of observation with the law of gravity, has been called NES (Natural Energy Surplus) [1].

The NES concept stems from known laws of physics, therefore any results obtained with it are unambiguously defined by these laws. It predicts an increase in velocity of matter bound by gravity to any structure. It displays some similarities to the MOND concept (Milgrom 1983) through compliance of the r_k parameter appearing in NES (which is named here as Kepler's radius), with the r_t - transition radius (Milgrom 1983) or r_M - MOND radius (e.g. Milgrom 2010a, 2012a). This, in turn, suggests that acceleration A appearing in NES is equivalent to MOND acceleration a_0 (e.g. Milgrom 2011).

However, unlike MOND, NES indicates that it is possible to explain the observations non-compliance with the Newton's law of gravity through a physical mechanism, that is based on the well-known laws. Unlike MOND, it also suggests meaning and significance of acceleration a_0 through meaning and significance of acceleration A. From the concept of the NES also follows a more complex relation between mass and terminal rotation velocity in spiral galaxies which, however, for the point mass, takes form similar to the one resulting from MOND.

Because the additional particle velocity resulting from NES depends only on Newtonian potential defined by distribution of baryonic mass, we can determine this velocity, basing on the baryonic rotation curve of this distribution. This means that no additional non-baryonic mass is needed to explain the observed increase in particle velocity.

2. NES Rotation

The observed circular velocity of a particle in a gravitational field of a spherical mass distribution, takes the following form in NES:

$$v_{c_{nes}}^2 = v_c^2 + v_{ex}^2, \tag{1}$$

where: $v_{c_{nes}}$ is NES rotation, v_c is Newtonian rotation and v_{ex} is an additional rotation appearing in NES (extra rotation velocity of particle), which takes the following form:

$$v_{ex} = f(\Phi_N), \tag{2}$$

[1] will be presented in a separate publication

where Φ_N is Newtonian potential.
Note that formula (1) resembles the well-known formula for observed rotation in spiral galaxies with dark matter halo influence taken into account (e.g. de Blok et al. 2008):

$$v_{obs}^2 = v_c^2 + v_{halo}^2, \quad \text{where:} \quad v_c^2 = V_{gas}^2 + \Upsilon_* V_*^2. \tag{3}$$

For a field that originates from point mass, from formula (1) we obtain:

$$v_{c_{nes}}^2 = \frac{A r_k^2}{r} + v_{ex}^2, \tag{4}$$

wherein v_{ex}^2 is then equal to:

$$v_{ex}^2 = \frac{A\, r_k}{2\sqrt{2}} \left[\frac{1}{2} \ln \left(\frac{r^2}{r_k^2} - \sqrt{2}\, \frac{r}{r_k} + 1 \right) - \frac{1}{2} \ln \left(\frac{r^2}{r_k^2} + \sqrt{2}\, \frac{r}{r_k} + 1 \right) + \arctan \left(\sqrt{2}\, \frac{r}{r_k} + 1 \right) + \arctan \left(\sqrt{2}\, \frac{r}{r_k} - 1 \right) \right], \tag{5}$$

where: $r_k = \sqrt{\mathrm{G}M/A}$ is Kepler's radius for M mass, G - gravitational constant, M - mass of the point mass.
For $r/r_k \ll 1$, Eq. (4) takes the known form:

$$v_{c_{nes}}^2 = \frac{A r_k^2}{r} = \frac{\mathrm{G}M}{r} = v_c^2. \tag{6}$$

Taking (4) and (5) into account, we obtain the terminal rotation velocity around the point mass:

$$v_\infty = \sqrt{\frac{\pi A\, r_k}{2\sqrt{2}}} = \left(\frac{\pi^2}{8} A \mathrm{G} M \right)^{1/4}. \tag{7}$$

Figure 1 presents a graph of relations (4) for an exemplary point mass equal to the mass of the Galaxy (Sofue et al. 2009). As seen on the graph, the NES rotation can be conventionally divided into two areas: Keplerian, for $r < r_k$, and non-Keplerian for $r > r_k$. r_k can thus be regarded as radius of the Keplerian area. Formula (7) indicates that the terminal value of NES rotation is defined by extra rotation v_{ex} and, for the assumed value of mass, the v_∞ matches the Galaxy's terminal rotation value (Sofue et al. 2009). v_{ex} graph is noteworthy - its shape resembles dark matter halo contribution that results from the ISO model (e.g.

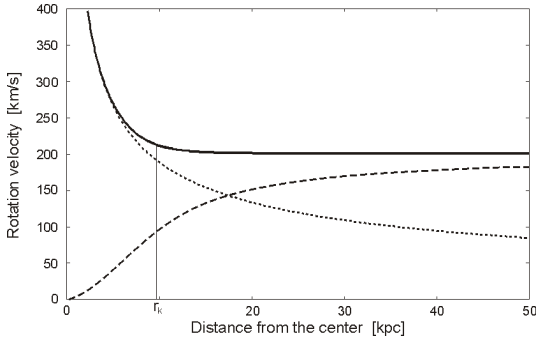

Fig. 1.— Theoretical NES rotation around a point mass of exemplary mass $M = 8,3 \times 10^{10} M_\odot$ (mass of the Galaxy) - thickline; dotted line - Keplerian rotation; dashed line - v_{ex} extra rotation, establishing the terminal rotation for this mass at 200 $\frac{\mathrm{km}}{\mathrm{s}}$.

McGaugh 2004; de Blok & Bosma 2002).
From the Eq. (7) we obtain the relation between the point mass M and the terminal rotation velocity around mass M:

$$M = q\, v_\infty^4, \tag{8}$$

where:

$$q = \frac{8}{\pi^2\, A\, \mathrm{G}} \approx \frac{0.81}{A\, \mathrm{G}}, \tag{9}$$

which, depending on the adopted A value, gives:

$$q_{(A=1.2\times10^{-10}\ \frac{\mathrm{m}}{\mathrm{s}^2})} \approx 51 \left[\frac{\mathrm{M}_\odot\, \mathrm{s}^4}{\mathrm{km}^4} \right], \tag{10}$$

$$q_{(A=1.3\times10^{-10}\ \frac{\mathrm{m}}{\mathrm{s}^2})} \approx 47 \left[\frac{\mathrm{M}_\odot\, \mathrm{s}^4}{\mathrm{km}^4} \right]. \tag{11}$$

Note that mass' dependence on terminal velocity in relation to (8) has the same form as an empirical baryonic Tully-Fisher relation (BTFR) (McGaugh 2012), and that the value of the coefficient (10) and (11) corresponds with the value of this coefficient indicated in BTFR:

$$q_{BTFR} = 47 \pm 6 \left[\frac{\mathrm{M}_\odot\, \mathrm{s}^4}{\mathrm{km}^4} \right]. \tag{12}$$

Assuming $r/r_k = p$, the following ratio results from equations (4) and (5):

$$\frac{v_{c_{nes}}^2}{v_c^2}(p) = \frac{M_{ef}}{M}(p) = 1 + \frac{p}{2\sqrt{2}} \left[\frac{1}{2} \ln \left(p^2 - \sqrt{2}\, p + 1 \right) \right.$$

$$- \frac{1}{2}\ln\left(p^2+\sqrt{2}\,p+1\right)+\arctan\left(\sqrt{2}\,p+1\right)$$
$$+\arctan\left(\sqrt{2}\,p-1\right)\Bigg], \qquad (13)$$

where M_{ef} is the effective mass necessary to induce the same circular velocity (or escape velocity) of the particle that stems from NES.
In Figure 2 we can see the graph of relations (13), whose shape resembles a hockey stick. A similar shape has been revealed in dynamical mass over detected mass relation, but in a_0/a function of MOND concept (Milgrom 1999). Writing down

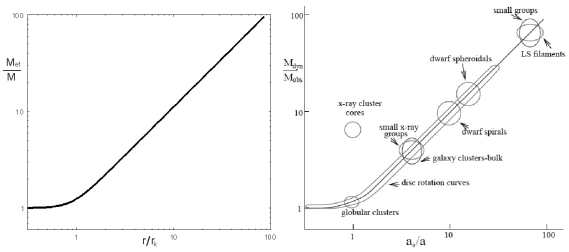

Fig. 2.— Left: graph of relations resulting from formula (13); right: graph revealing itself in MOND concept.

the relation (13) as a function of Newton's acceleration $g_N = v_c^2/r = Ar_k^2/r^2$, we obtain:

$$\frac{v_{c_{nes}}^2}{v_c^2}(g_N) = 1+\frac{1}{2\sqrt{2}}\sqrt{\frac{A}{g_N}}\left[\frac{1}{2}\ln\left(\frac{A}{g_N}-\sqrt{\frac{2A}{g_N}}+1\right)\right.$$
$$-\frac{1}{2}\ln\left(\frac{A}{g_N}+\sqrt{\frac{2A}{g_N}}+1\right)$$
$$+\arctan\left(\sqrt{\frac{2A}{g_N}}+1\right)$$
$$\left.+\arctan\left(\sqrt{\frac{2A}{g_N}}-1\right)\right]. \qquad (14)$$

Figure 3 shows relation (14) graph drawn over V^2/V_b^2 graph, where V is the observed velocity and V_b is the velocity attributable to visible baryonic matter in Newton's acceleration function $g_N = V_b^2/r$, resulting from hundreds of measurements taken for nearly a hundred spiral galaxies (Famaey & McGaugh 2012).

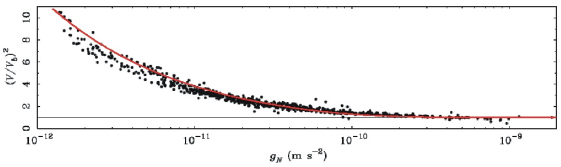

Fig. 3.— Graph of $(v_{c_{nes}}/v_c)^2\,(g_N)$ relations for point mass (red line), drawn over a graph of $(V/V_b)^2\,(g_N)$ relations, resulting from hundreds of measurements taken for nearly a hundred spiral galaxies. Based on (Famaey & McGaugh 2012).

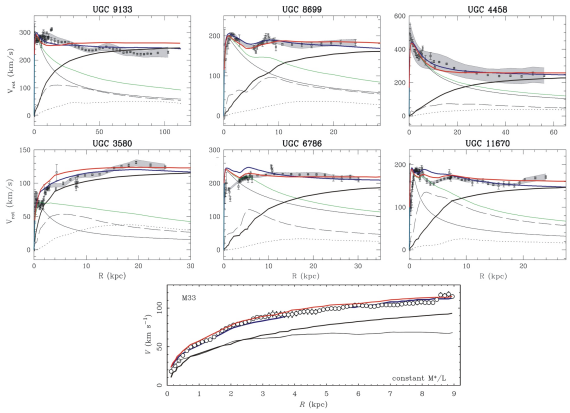

Fig. 4.— NES rotation curves determined for exemplary spiral galaxies - red line. Observed rotation - gray strip (M33 - circles). Extra rotation - thick black line. Resultant baryonic rotation - thin green line (M33 - thin black line). All other markings as described in (Milgrom 2010b; Famaey & McGaugh 2012).

In order to determine the NES rotation for mass distribution and to compare it with rotation observed for such distribution, examples of spiral galaxies have been used, with calculated observed rotation curves and rotation from baryonic mass (Newtonian rotation) - essential for NES formulas. Unfortunately, due to the method of determining baryonic mass in galaxies, we are not sure if the rotation curve for such mass has been calculated correctly. NES rotation is based on it, so this makes verifying the correctness of determined NES rotation harder. In Figure 4 we can see several examples of NES rotations designated numerically, drawn over graphs of galaxies' rotations, coming from (Milgrom 2010b; Famaey & McGaugh 2012). After numerically determining

v_{ex} extra rotation from formula (2), the NES rotation has been determined from formula (1).

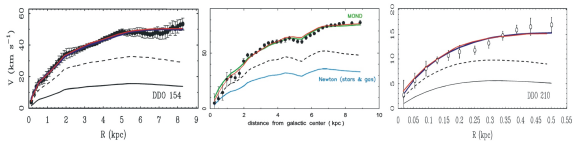

Fig. 5.— Baryonic rotation curve suggested by NES (dashed line) that provides similar compliance of NES and MOND rotation curves for three examples of galaxies, for which: $g_{N_{max}} \ll A$: on the left - DDO 154, in the middle - NGC 1560, on the right - DDO 210. NES rotation curves - red line. All other markings as described in (Famaey & McGaugh 2012; Milgrom 2012b).

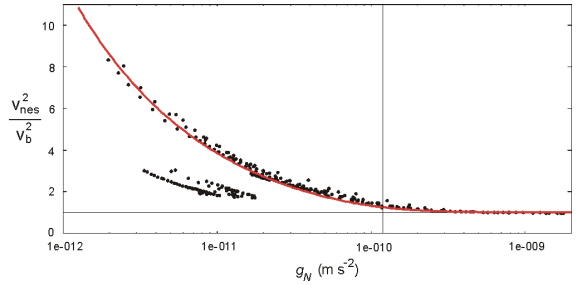

Fig. 6.— Graph of $v^2_{c_{nes}}/v^2_b$ relations in Newton's acceleration function g_N, resulting from around three hundred measurements, taken for ten exemplary galaxies. A different location can be seen for three galaxies, for which $g_{N_{max}} \ll A$. The red line corresponds to graph of this relation for point mass. Original baryonic rotations for galaxies from Fig. 4 and those suggested by NES for Fig. 5 galaxies have been used for calculations.

NES shows that, for galaxies in which the maximum centripetal acceleration of mass rotating around center is significantly smaller than A, the connection between terminal velocity and baryonic mass is weaker than for point mass and for other cases (e.g. Galaxy). Due to this, terminal velocities for such galaxies are smaller than for point masses of corresponding mass. This means that in order to reach the same terminal velocity the mass of such galaxy has to be greater than the mass of point mass. DDO 154 and NGC 1560 are examples of such galaxies. The compliance of NES rotation with the one observed can be achieved for masses greater than the one assumed. Figure 5 shows baryonic rotations suggested by NES for three such galaxies, that provide similar compliance of NES and MOND rotations.

Figure 6 presents a graph of $v^2_{c_{nes}}/v^2_b$ relations in Newton's acceleration function $g_N = v^2_b/r$, for ten galaxies shown in Figs. 4 and 5. According to NES, the galaxies in which the maximum centripetal acceleration of mass rotating around center is significantly smaller than A, should be localized under the main branch of the graph, that corresponds to other cases, including the point mass case.

Figure 7 presents a graph of relations between baryonic mass and NES terminal rotation for galaxies from Figs. 4 and 5 drawn over (McGaugh 2012) BTFR relations graph. The straight red line is a point mass graph resulting from Eq. (8) for $A = 1.2 \times 10^{-10}$ m/s^2:

$$\log M = 4 \log v_\infty + 1.7. \qquad (15)$$

3. Conclusions

All results presented in this paper are a consequence of a physical mechanism described by known laws. Therefore, their similarity to the observed results seems like an important argument for further verification of this concept and its predictions.

REFERENCES

de Blok, W. J. G. & Bosma, A. 2002, A&A, 385, 816

de Blok, W. J. G., Walter, F., Brinks, E., et al. 2008, AJ, 136, 2648

Famaey, B. & McGaugh, S. S. 2012, Living Reviews in Relativity, 15, 10

McGaugh, S. S. 2004, ApJ, 609, 652

McGaugh, S. S. 2012, The Astronomical Journal, 143, 40

Milgrom, M. 1983, ApJ, 270, 365

Milgrom, M. 1999, in Dark matter in Astrophysics and Particle Physics, ed. H. V. Klapdor-Kleingrothaus & L. Baudis, 443

Milgrom, M. 2010a, MNRAS, 405, 1129

Milgrom, M. 2010b, in American Institute of Physics Conference Series, Vol. 1241, American Institute of Physics Conference Series, ed. J.-M. Alimi & A. Fuözfa, 139–153

Milgrom, M. 2011, ArXiv e-prints

Milgrom, M. 2012a, MNRAS, 426, 673

Milgrom, M. 2012b, ArXiv e-prints

Rubin, V. C., Thonnard, N., & Ford, Jr., W. K. 1978, ApJ, 225, L107

Sofue, Y., Honma, M., & Omodaka, T. 2009, PASJ, 61, 227

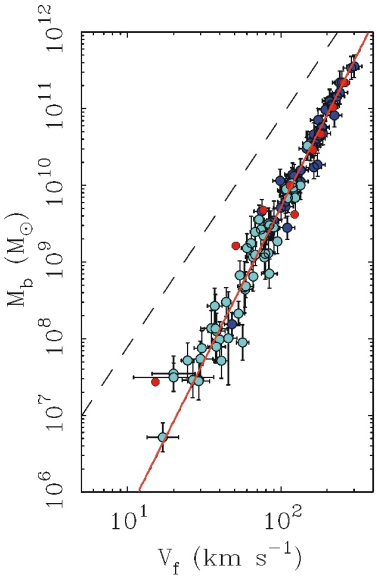

Fig. 7.— Graph of relations between baryonic mass and NES terminal rotation for ten exemplary galaxies (red circles) drawn over (Famaey & McGaugh 2012) BTFR relations graph. The straight red line is a point mass graph resulting from Eq. (15). Original baryonic rotations for galaxies from Fig. 4 and those suggested by NES for Fig. 5 galaxies have been used for calculations. All other markings as described in (Famaey & McGaugh 2012).

This 2-column preprint was prepared with the AAS LaTeX macros v5.2.